

Prediction of Maximum Moment of Rectangular Tubes Subjected to Pure Bending

K. Masuda and D. H. Chen

Department of Mechanical Engineering, Tokyo University of Science, 1-3 Kagurazaka, Shinjuku-ku, Tokyo, 162-8601, Japan

Abstract *In this paper, the collapse behaviors of rectangular tube subjected to pure bending are studied by using the finite element method. Such bending collapse has been studied for a long time, including the landmark study by Kecman. According to these studies, there are two types of collapses. The first type is a collapse due to buckling at the compression flange. The second type is a collapse due to plastic yielding at the flanges. However, there may be another collapse. For a rectangular tube in which the web is wider than the flange, it is found that collapse due to buckling at the compression web may occur. Further, an approximation prediction method is proposed for estimating the maximum bending moment of rectangular tubes in which the web buckling is also taken into account. Its validity is verified by comparing with the numerical results by FEM under various conditions.*

Keywords *FEM, Pure bending, Rectangular tube, Buckling, Effective width*

1. Introduction

Evaluation of a car's crush behavior when the car is subjected to an oblique load, such as in an offset crash, is becoming increasingly important for general car design. It is thus vital to understand the crushing characteristic of rectangular tubes that are used as general components in car. Because the oblique load can be decomposed into axial load and pure bending, the pure bending of the rectangular tubes has been widely studied for a long time^[1, 2, 3], including the landmark study by Kecman^[1]. According to these studies, there are two types of collapses. The first type is a collapse due to buckling at the compression flange. The second type is a collapse due to plastic yielding at the flanges. However, when the web is wider than the flange, it is considered that a collapse due to buckling at the compression web may occur because it was already reported in bending of open section beams^[4].

In the present study, the effects of the material and geometrical properties of rectangular tubes on their bending collapse are studied by using the finite element method. Further, based on the numerical results obtained, a method for estimating the maximum bending moment of rectangular tubes subjected to pure bending is proposed.

In addition, a validity of FE analysis result under bending collapse has been already verified by comparing the experimental results by Kyriakides^[5] with the previous numerical results by authors^[6] under pure bending with cylindrical tubes.

2. Analytical method

The commercial FEM analysis package MSC. Marc^[7] is used in this study to analyze large elastoplastic bending of the rectangular tubes shown in Fig. 1. In the present calculation, one end of the rectangular tube was completely fixed to a rigid wall. Pure bending was applied from the other end by modeling a lid rotating about the axis of z under rotary control. The effects of various geometric parameters, such as tube thickness t , tube flange width c_1 , and tube web width c_2 , on the bending collapse were investigated. The value of lid thickness t_f was set to five times t as referred to Guarracino^[8] because the lid must be stiff enough to prevent distortion.

The tube material used in the analysis was assumed to be homogeneous and isotropic elastic perfectly plastic material that conforms to von Mises yield conditions. In this study, it was assumed that Young’s modulus $E = 72.4$ GPa, and Poisson’s ratio $\nu = 0.3$. The influence of the material properties on the bending collapse of the rectangular tube was investigated in terms of the yield stress σ_y .

In this study, the updated Lagrange method was used to formulate the geometric nonlinear behavior, and the algorithm based on the Newton-Raphson method and the return-mapping method were used to solve the nonlinear equation. The rectangular tubes were modeled using four-node quadrilateral thickness shell elements (Element type 75). The elements were divided the flange and web width into 20 sub lengths, and divided the axial length in a way that the elements become almost square.

In addition, the rectangular length used in the analysis was assumed to be long enough in order to exclude the influence of the boundary conditions. The ratio of the length and flange width L/c_1 was set to $L/c_1 > 6$.

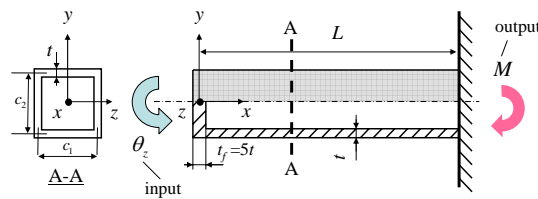


Fig.1. Tube geometry and loading condition

3. Results and discussion

3.1 Comparison between proposal method by Kecman and results of present numerical analyses

First, we show Kecman’s method for estimating the maximum bending moment of rectangular tubes subjected to pure bending. For a rectangular tube subjected to pure bending, the buckling stress σ_{buc} of the compression flange was derived in the following equation.

$$\sigma_{buc} = \frac{\pi^2 E}{12(1-\nu^2)} \left(5.23 + 0.16 \frac{a}{b} \right) \left(\frac{t}{a} \right)^2 \tag{1}$$

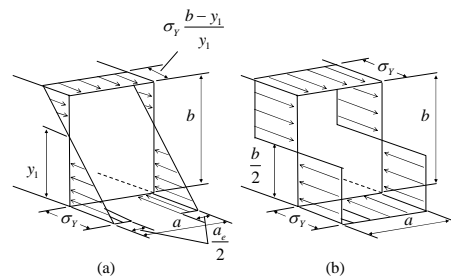


Fig.2. Schematic representation of axial stress distribution proposed by Kecman: (a) $\sigma_{buc} < \sigma_y$; (b) $\sigma_{buc} \geq 2\sigma_y$

where E , ν , a , b , and t are respectively, Young’s modulus, Poisson’s ratio, flange width, web width and tube thickness. In addition, a is $c_1 + t$ and b is $c_2 + t$.

Kecman presented a proposal method in which was decided by relations of the buckling stress σ_{buc} and yield stress σ_y .

(1) In the case of $\sigma_{buc} < \sigma_y$

If the buckling stress σ_{buc} is less than the yield stress σ_y , the compression flange buckles

and the edges stress come up to yield stress σ_y . In order to consider this phenomenon, an effective width σ_e is introduced in the following simplified equation.

$$a_e = a \left(0.7 \frac{\sigma_{buc}}{\sigma_y} + 0.3 \right) \tag{2}$$

As a result, stress distribution in the maximum moment is shown in Fig. 2(a). In the figure, y_1 in which the distances from a compression flange to the neutral axis is derived from the condition of zero axial loads. Therefore, y_1 is given by the following equation.

$$\frac{y_1}{b} = \frac{a+b}{a_e+a+2b} \tag{3}$$

By summing moments through the cross-section, the maximum bending moment is derived in the following equation.

$$M_{\max} = \sigma_y \cdot t \cdot b^2 \cdot \frac{2a+b+a_e \cdot \left(3 \frac{a}{b} + 2 \right)}{3(a+b)} \tag{4}$$

(2) In the case of $\sigma_{buc} \geq 2\sigma_y$

In this case, stress distribution in the maximum moment is shown in Fig. 2(b). Namely, it is assumed that the maximum moment is equal to a fully plastic moment M_p . The maximum bending moment is derived in the following equation.

$$M_{\max} = M_p = \sigma_y \cdot t \left[a(b-t) + 0.5(b-2t)^2 \right] \tag{5}$$

(3) In the case of $\sigma_y \leq \sigma_{buc} < 2\sigma_y$

First, if the buckling stress σ_{buc} is equal to the yield stress σ_y , it is assumed that the maximum moment is equal to a elastic moment M_e in which the stress of flanges are equal to the yield stress σ_y . This elastic moment M_e is derived in the following equation.

$$M_e = \sigma_y \cdot t \cdot b \cdot \left(a + \frac{b}{3} \right) \tag{6}$$

And in the case of $\sigma_y \leq \sigma_{buc} < 2\sigma_y$, the maximum bending moment is derived from linear interpolation:

$$M_{\max} = M_e + (M_p - M_e) \frac{\sigma_{buc} - \sigma_y}{\sigma_y} \tag{7}$$

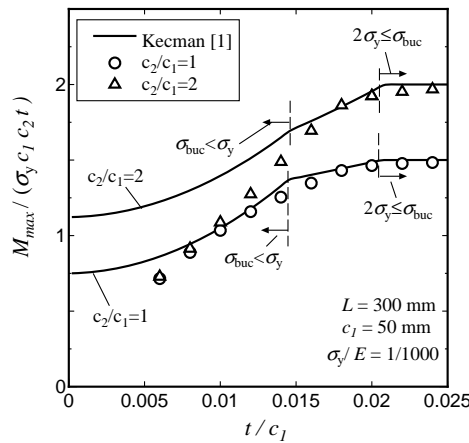


Fig.3. Comparison between Kecman’s proposal and results of FEM with relation of t/c_1 and $M_{\max} / (\sigma_y \cdot c_1 \cdot c_2 \cdot t)$

Figure 3 compares these proposal methods by Kecman and results of present numerical analyses for two levels of aspect ratio c_2/c_1 with $c_1=50\text{mm}$, $L=300\text{mm}$, $\sigma_y/E=0.001$. As can be seen from this figure, in the case of high-aspect ratio in which the web is wider than the flange, the results of maximum moment under various t/c_1 between the Kecman's proposal and results of FEM have a margin of error. In particular, the error increases with decreasing t/c_1 . Therefore, it is found that a region which does not apply to Kecman's proposal exists. In order to estimate the maximum moment, it is vital to reveal the bending collapse mechanism of rectangular tubes.

3.2 Two types of collapse mechanism pointed out by Kecman

An investigation of two types of collapse mechanism pointed out by Kecman was presented by using square tubes in which the aspect ratio c_2/c_1 was set to 1. Figure 4 shows the relation of a tube curvature $\kappa = \theta/L$ and moment M for a square tube with $t=0.9\text{mm}$, $c_1=50\text{mm}$, $c_2=50\text{mm}$, $\sigma_y/E=0.001$ ($\sigma_{buc}=1.52\sigma_y$). And figure 4 also shows the relations of the tube curvature $\kappa = \theta/L$ and axial stress σ_x/σ_y at point B and C (refer to schematic representation of cross-section in figure 4). As can be seen from the figure, the maximum moment is in good agreement with the value of Kecman's proposal equation (7). The axial compression stress σ_x/σ_y at point B in the middle of compression flange increases until the moment becomes maximum moment, and the value σ_x/σ_y comes up to 1. In addition, the axial compression stress σ_x/σ_y at point C in the quarter of web width increases until the moment becomes maximum moment. Figure 5 shows the axial stress distribution of cross-section at phase (α) and (β) corresponding to $\theta/L=0.025\text{m}^{-1}$ and 0.065m^{-1} in Fig. 4. As can be seen from the figure, the absolute value of the axial stress when the maximum moment occurs is greater than the value at phase (α) in all cross-section positions. In addition, the axial stress distribution when the maximum moment occurs is in good agreement with Kecman's proposal. It is confirmed from the above investigation that in the case of $c_2/c_1=1$ and $\sigma_y \leq \sigma_{buc}$, the collapse type is not due to buckling at the compression flange and web, but due to plastic yielding at the flanges. Therefore, to estimate the maximum moment by Kecman's theory is possible in this case.

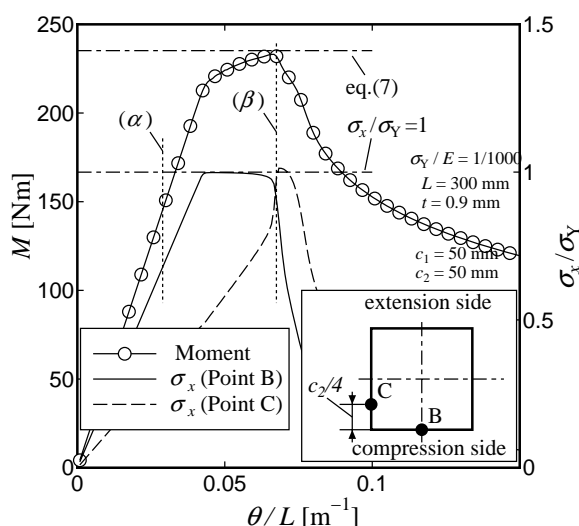


Fig.4. Relations of θ/L and $M, \sigma_x/\sigma_y$ for square tube with $t=0.9\text{mm}$, $c_1=50\text{mm}$, $c_2=50\text{mm}$

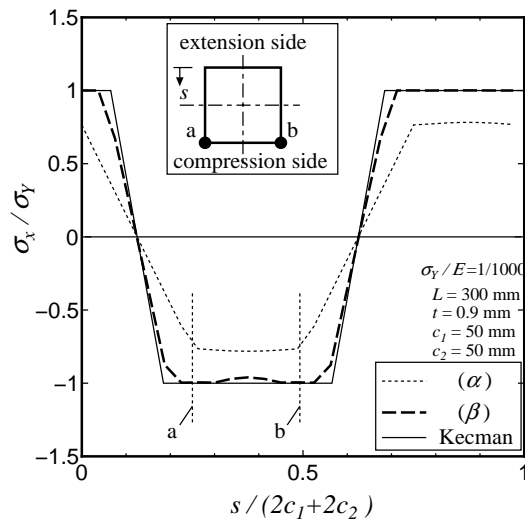


Fig.5. Axial stress distribution of cross-section for the square tube shown in Fig.4

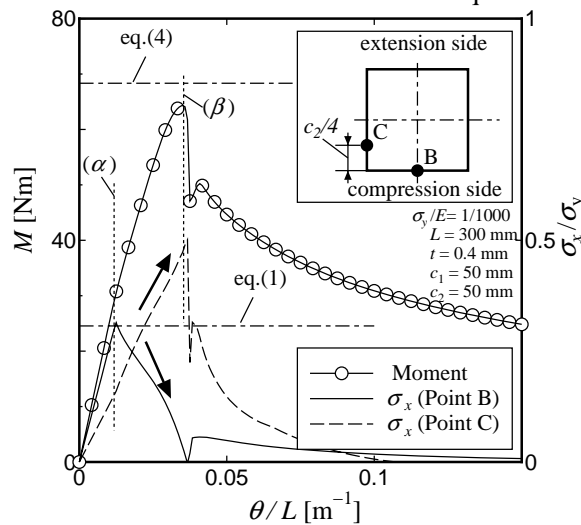


Fig.6. Relations of θ/L and $M, \sigma_x/\sigma_y$ for square tube with $t=0.4\text{mm}$, $c_1=50\text{mm}$, $c_2=50\text{mm}$

Figure 6 shows the relation of a tube curvature $\kappa = \theta/L$ and moment M for a square tube with $t=0.4\text{mm}$, $c_1=50\text{mm}$, $c_2=50\text{mm}$, $\sigma_y/E = 0.001$ ($\sigma_{buc} = 0.31\sigma_y$). And figure 6 also shows the relations of the tube curvature $\kappa = \theta/L$ and axial stress σ_x/σ_y at point B and C (refer to schematic representation of cross-section in figure 6). As can be seen from the figure, the maximum moment is in good agreement with the value of Kecman's proposal equation (4). The axial compression stress σ_x/σ_y at point B in the middle of compression flange decreases before the moment becomes maximum moment, and the maximum value σ_x/σ_y is in good agreement with the equation (1) of elastic buckling stress. In addition, the axial compression stress σ_x/σ_y at point C in the quarter of web width increases until the moment becomes maximum moment. Figure 7 shows the axial stress distribution of cross-section at phase (α) and (β) corresponding to $\theta/L = 0.012\text{m}^{-1}$ and 0.038m^{-1} in Fig. 6. As can be seen from the figure, although the axial compression stress in the middle of compression flange decreases due to buckling in the middle of compression flange, the axial compression stress in both edges

of compression flange increase because buckling doesn't occur in both edges. Immediately after buckling, stress increment in the both edges is greater than stress decrement in the middle of compression flange. Therefore, total force of compression side and moment increase. In addition, the stress distribution of the web changes linearly because buckling doesn't occur in the web. Therefore, the axial stress distribution when the maximum moment occurs is in good agreement with Kecman's proposal by using an effective width in the compression flange. It is confirmed from the above investigation that in the case of $c_2/c_1=1$ and $\sigma_y > \sigma_{buc}$, the collapse type is due to buckling at the compression flange. Therefore, to estimate the maximum moment by Kecman's theory is possible in this case.

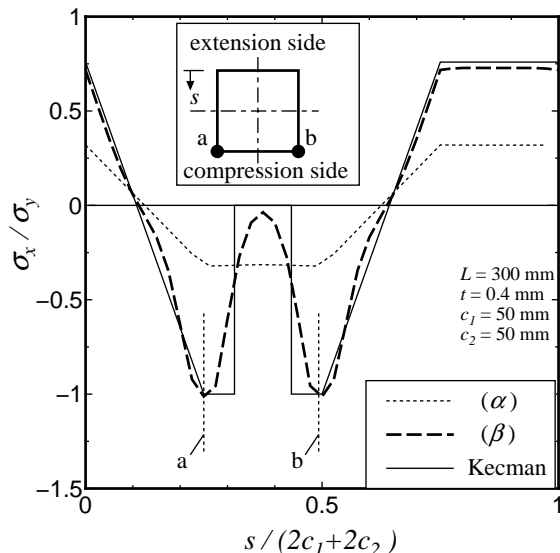


Fig.7. Axial stress distribution of cross-section for the square tube shown in Fig.6

3.3 Collapse mechanism which is different from Kecman's indication

In the case of high-aspect ratio in which the web is wider than the flange, it was confirmed that collapse due to buckling at the compression web occur.

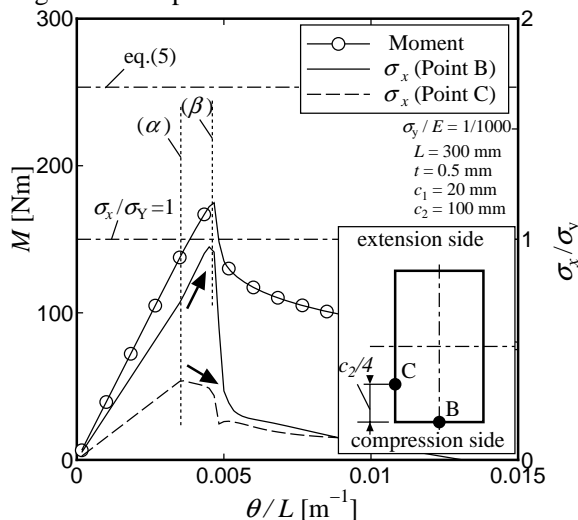


Fig.8. Relations of θ/L and $M, \sigma_x/\sigma_y$ for rectangular tube with $t=0.5\text{mm}$, $c_1=20\text{mm}$, $c_2=100\text{mm}$

Figure 8 shows the relation of a tube curvature $\kappa = \theta/L$ and moment M for a rectangular tube with $t=0.5\text{mm}$, $c_1=20\text{mm}$, $c_2=100\text{mm}$, $\sigma_y/E = 0.001$ ($\sigma_{buc} = 2.83\sigma_y$, $c_2/c_1 = 5$). And figure 8 also shows the relations of the tube curvature $\kappa = \theta/L$ and axial stress σ_x/σ_y at point B and C (refer to schematic representation of cross-section in figure 8). As can be seen from the figure, the maximum moment is less than the value of Kecman's proposal equation (5). In addition, the axial compression stress σ_x/σ_y at point B in the middle of compression flange increases until the moment becomes maximum moment, and the value σ_x/σ_y comes up to 1. And the axial compression stress σ_x/σ_y at point C in the quarter of web width decreases before the moment becomes maximum moment. Figure 9 shows the axial stress distribution of cross-section at phase (α) and (β) corresponding to $\theta/L = 0.036\text{m}^{-1}$ and 0.048m^{-1} in Fig. 8. As can be seen from the figure, the axial stress distribution in the compression flange is constant value and the absolute value is almost 1 when the maximum moment occurs. And the axial stress distribution in the compression web doesn't increase linearly. Therefore, the sum of axial stress when the maximum moment occurs is less than the Kecman's proposal as much as it is shown by arrows of Figure 9.

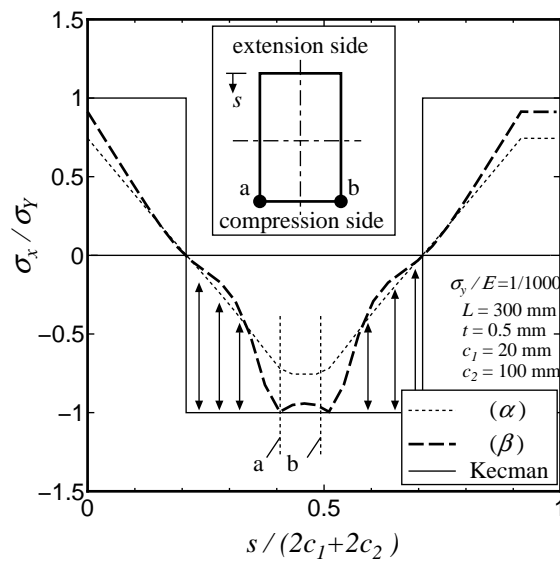


Fig.9. Axial stress distribution of cross-section for the rectangular tube shown in Fig.8

It is found from the above investigation that in the case of high-aspect ratio and $\sigma_y < \sigma_{buc}$, the collapse type is not due to buckling at the compression flange but due to buckling at the compression web. Therefore, to estimate the maximum moment by Kecman's theory is impossible in this case.

Figure 10 shows the relation of a tube curvature $\kappa = \theta/L$ and moment M for a rectangular tube with $t=0.4\text{mm}$, $c_1=50\text{mm}$, $c_2=100\text{mm}$, $\sigma_y/E = 0.001$, ($\sigma_{buc} = 0.30\sigma_y$), ($c_2/c_1 = 2$). And figure 10 also shows the relations of the tube curvature $\kappa = \theta/L$ and axial stress σ_x/σ_y at point B and C (refer to schematic representation of cross-section in figure 10). As can be seen from the figure, the maximum moment is less than the value of Kecman's proposal equation (4). The axial compression stress σ_x/σ_y at point B in the middle of compression flange decreases before the moment becomes maximum moment, and the maximum value σ_x/σ_y is in good agreement with the equation (1) of elastic buckling stress. In addition, the axial compression stress σ_x/σ_y at point C in the quarter of web width decreases before the moment becomes

maximum moment. Figure 11 shows the axial stress distribution of cross-section at phase (α) and (β) corresponding to $\theta/L = 0.007m^{-1}$ and $0.016m^{-1}$ in Fig. 10. As can be seen from the figure, the axial stress in the compression flange is concentrated in the edges when the maximum moment occurs. And the axial stress distribution in the compression web doesn't increase linearly. Therefore, the sum of axial stress in the maximum moment is less than the Kecman's proposal as much as it is shown by arrows of Figure 11 because the equation (2) applies to the axial stress distribution of compression flange, and linearly approximation doesn't apply to the axial stress distribution of compression web. It is found from the above investigation that in the case of high-aspect ratio and $\sigma_y \geq \sigma_{buc}$, the collapse type is not only due to buckling at the compression flange but also due to buckling in the compression web. Therefore, to estimate the maximum moment by Kecman's theory is impossible in this case.

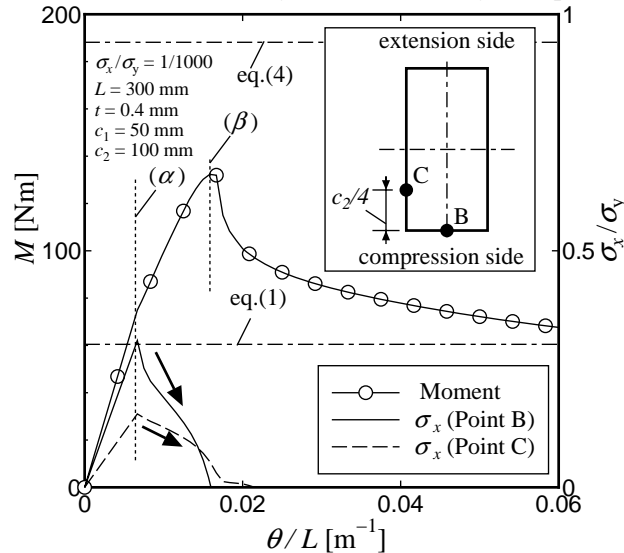


Fig.10. Relations of θ/L and $M, \sigma_x/\sigma_y$ for rectangular tube with $t=0.5$ mm, $c_1=20$ mm, $c_2=100$ mm

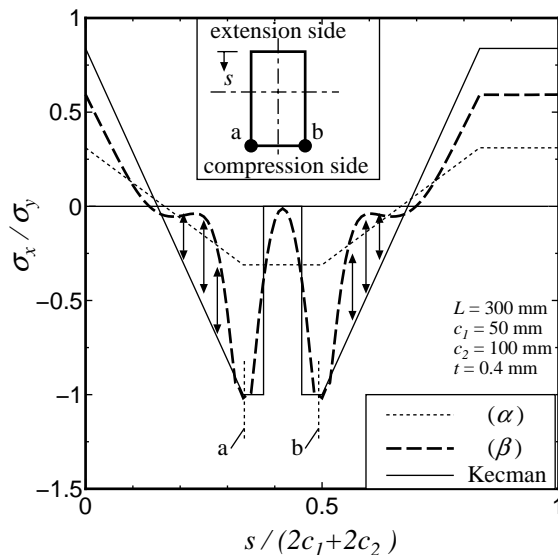


Fig.11. Axial stress distribution of cross-section for the rectangular tube shown in Fig.10

3.4 Proposal method of maximum moment considering the web buckling

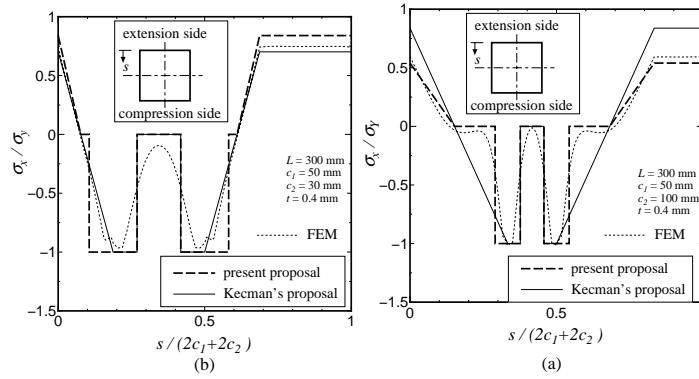


Fig.12. Axial stress distribution in the range of $\sigma_{buc} < \sigma_y$: (a) by Kecman's method; (b) by present method

Figure 12 shows a schematic representation of axial stress distribution in the maximum moment after buckling of the compression flange ($\sigma_{buc} < \sigma_y$). Figure 12(a) shows Kecman's proposal in which doesn't consider the web buckling, and figure 12(b) shows present proposal in which considers the web buckling. As can be seen in the figure(b), an effective width a_e applies to the compression web as well as the compression flange. It is assumed that the effective width a_e is independent of initial web width as referring to Karman's theory^[9]. A coefficient α in which represents the axial tension stress is derived in the following equation.

$$\alpha = \frac{2(a_e - t)}{a + b - y_1 - 2t} \tag{8}$$

Figures 13(a) and (b) show comparison between results of FEM and proposals with the axial stress distribution. As can be seen in the figures, in the case of high-aspect ratio $c_2/c_1 = 2$, present proposal in which considers the web buckling is in good agreement with the result of FEM. And in the case of low-aspect ratio $c_2/c_1 = 0.6$, Kecman's proposal in which doesn't consider the web buckling is in good agreement with the result of FEM.

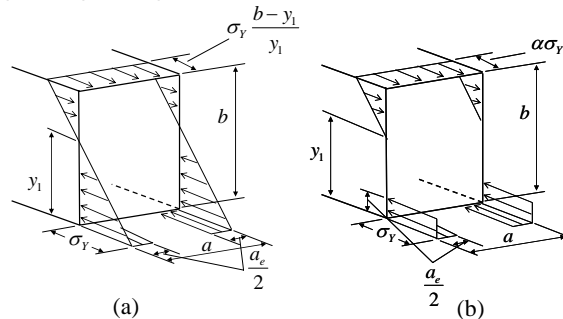


Fig.13. Axial stress distribution by results of FEM, Kecman's proposal and present proposal: with (a) $c_2/c_1 = 2$; (b) $c_2/c_1 = 0.6$

Figure 14 shows a schematic representation of axial stress distribution in the maximum moment when the compression flange doesn't buckle ($\sigma_{buc} \geq \sigma_y$). Figure 14(a) shows Kecman's proposal in which doesn't consider the web buckling, and figure 14(b) shows present proposal in which considers the web buckling. As can be seen in the figure, an effective width a_e applies to only the compression web. A coefficient β in which represents the axial tension stress is derived in the following equation.

$$\beta = \frac{a + a_e - 2t}{a + b - y_1 - 2t} \tag{9}$$

Figures 15(a) and (b) show comparison between results of FEM and proposals with the axial stress distribution. As can be seen in the figures, in the case of high-aspect ratio $c_2/c_1 = 5$, present proposal in which considers the web buckling is in good agreement with the result of FEM. And in the case of low-aspect ratio $c_2/c_1 = 2$, Kecman's proposal in which doesn't consider the web buckling is in good agreement with the result of FEM.

We show present method for estimating the maximum bending moment of rectangular tubes subjected to pure bending. In the case of $\sigma_{buc} < \sigma_y$, a position of the center of gravity in the tension web G is derived in the following equation.

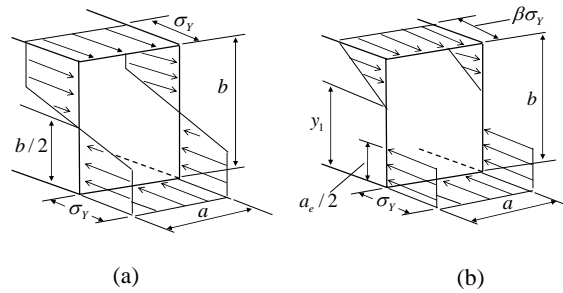


Fig.14. Axial stress distribution in the range of $\sigma_{buc} \geq \sigma_y$: (a) by Kecman's method; (b) by present method

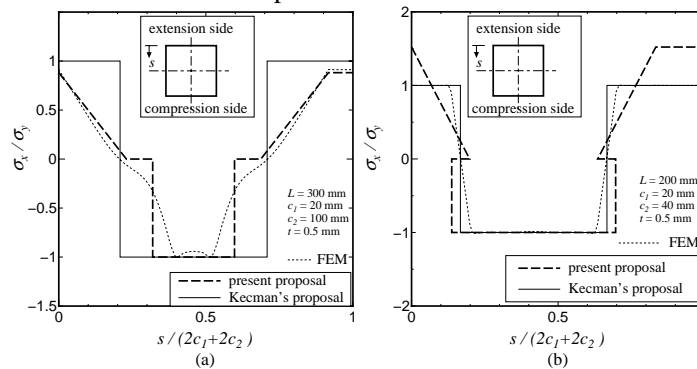


Fig.15. Axial stress distribution by results of FEM, Kecman's proposal and present proposal: with (a) $c_2/c_1 = 5$; (b) $c_2/c_1 = 2$

$$G = \frac{1}{3} \left(\frac{1}{2}b + y_1 \right) \tag{10}$$

Therefore, in the case of $\sigma_{buc} < \sigma_y$, the maximum moment in which the compression web buckles is derived in the following equation.

$$M_{\max} = \frac{1}{2} \sigma_y t \left\{ \alpha(a-2t)(b-t) + 2\alpha(b-y_1)G + (a_e-2t)(b-t) + 2a_e \left(\frac{b}{2} - \frac{a_e}{4} \right) \right\} \tag{11}$$

where y_1, α and G are respectively, the value of equation (3), (8) and (10). It is found from the above investigation that in the case of $\sigma_{buc} < \sigma_y$, the maximum moment is derived in the following equation.

$$M_{\max} = \text{Min}(\text{eq.(4)}, \text{eq.(11)}) \tag{12}$$

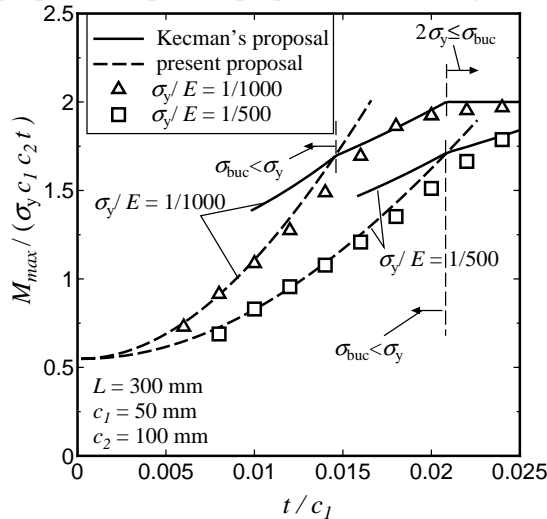
$$M_{\max} = \frac{1}{2} \sigma_y t \left\{ \beta(a-2t)(b-t) + 2\beta(b-y_1)G + (a-2t)(b-t) + 2a_e \left(\frac{b}{2} - \frac{a_e}{4} \right) \right\} \quad (13)$$

Moreover, in the case of $\sigma_{buc} \geq \sigma_y$, the maximum moment in which the compression web buckles is derived in the following equation.

where y_1, β and G are respectively, the value of equation (3), (9) and (10). It is found from the above investigation that in the case of $\sigma_{buc} \geq \sigma_y$, the maximum moment is derived in the following equation.

$$M_{\max} = \text{Min}(eq.(5), eq.(7), eq.(13)) \quad (14)$$

Figure 16 shows comparison between results of FEM and Kecman’s proposal and present proposal with the maximum moment for two levels of σ_y / E . As can be seen in the figure, the lower values of Kecman’s proposal and present proposal is in good agreement with the results of



FEM.

Comparison between results of FEM and Kecman’s proposal and present proposal with relation of t/c_1 and $M_{\max} / (\sigma_y \cdot c_1 \cdot c_2 \cdot t)$ for two levels of σ_y / E .

4. Conclusion

In this paper, the investigation of the bending collapse for rectangular tubes by using numerical analysis of the finite element method was presented. For a rectangular tube in which the web is wider than the flange, it is found that collapse due to buckling at the compression web may occur. It is possible to estimate the maximum moment under various the material and geometrical properties by using the present proposal in which applies an effective width to the web, and the Kecman’s proposal.

References

- [1] Kecman D. Bending collapse of rectangular and square section tubes, International Journal of Mechanical Sciences, Vol.25 (1983) 623-636.
- [2] Kim T. H. and Reid S. R. Bending collapse of thin-walled rectangular section columns, Computers and Structures, Vol.79 (2001) 1897-1911.
- [3] Lu G. and Yu T. X. Energy absorption of structures and materials, (2003) Section5 Crc Pr I Llc.
- [4] Parh M. S. and Lee B. C. Prediction of bending collapse behaviours of thin-walled open section beams, Thin-Walled Structures, Vol.25(3) (1996) 185-206.
- [5] Kyriakides S. and Ju G. T. Bifurcation and localization instabilities in cylindrical shells

- under bending, *International Journal of Solids and Structures*, Vol.29 (1992) 1117-1171.
- [6] Chen D. H. et al. Study on elastoplastic pure bending collapse of cylindrical tubes, *Transactions of the Japan Society of Mechanical Engineers, Series A*, Vol.74(740) (2008) 520-527.
- [7] MSC. Marc Manual, 2003.
- [8] Guarracino F. On the analysis of cylindrical tubes under flexure: theoretical formulations, experimental data and finite element analyses, *Thin-Walled Structures*, Vol.41 (2003) 127-147.
- [9] Karman V. T. et al. Strength of thin plates in compression, *Trans ASME*, Vol.54 (1932)